Sensitive and Efficient RF Harvesting Supply for Batteryless Backscatter Sensor Networks

Stylianos D. Assimonis, Spyridon-Nektarios Daskalakis, *Student Member, IEEE,* and Aggelos Bletsas, *Senior Member, IEEE*

Abstract—**This work presents an efficient and high sensitivity RF energy harvesting supply. The harvester consists of a single series circuit with one double diode on a low-cost, lossy FR-4 substrate, despite the fact that losses decrease RF harvesting efficiency. The design targeted minimum reflection coefficient *and* maximum rectification efficiency, taking into account not only the impedance matching network, but also the rectifier microstrip trace dimensions and the load. The simulated and measured rectenna efficiency was 28.4% for −20 dBm power input. In order to increase sensitivity, i.e. ability to harvest energy and operate at low power density, rectennas were connected in series configuration (voltage summing), forming rectenna arrays. The proposed RF harvesting system ability was tested at various input power levels, various sizes of rectenna arrays, with or without a commercial boost converter, allowing operation at RF power density as low as 0.0139 μW/cm^2. It is emphasized that the boost converter, whenever used, was self-started, without any additional external energy. The system was tested in supplying a scatter radio sensor, showing experimentally the effect of input power density on the operational cold start duration and duty cycle of the sensor.**

Index Terms—**Energy harvesting, rectifiers, rectennas.**

I. INTRODUCTION

EVEN though an ocean of electromagnetic waves surrounds us, most of that *ambient* electromagnetic energy remains unused. Moreover, the number of radio frequency (RF) emitters has been rapidly increasing over the last decades, due to the development of new wireless technologies such as cellular networks, wifi, digital TV and wireless sensor networks (WSN). Hence, there is an engineering challenge to collect unused ambient RF energy and supply with power small electrical devices, such as backscatter radio sensor networks [1]–[3]. Before three decades, William C. Brown proposed a system obtained from an antenna and a rectifier - the rectenna - for transformation of RF energy to dc [4]. Since then, RF energy harvesting has gained increasing interest, especially during the last years.

An important parameter in a rectenna system is the efficiency, i.e. the ratio of the dc power output to the RF power input. Nowadays, significant research effort has been directed towards high-efficiency rectennas. However, most prior art designs operate optimally at *high* input power, e.g. greater than 0 dBm [5]–[9]. In [5], an antenna array was used and efficiency was 65% for 25 dBm power input. In [6], authors

SND and AB are with School of Electronic and Computer Engineering (ECE), Technical University of Crete (TUC), GR-73100 Chania, Greece. SDA was with TUC, he is now with Physics Dept., Aristotle Univ. of Thessaloniki, GR-54124 Thessaloniki, Greece (e-mail: assimonis@physics.auth.gr; sdaskalakis@isc.tuc.gr; aggelos@telecom.tuc.gr).

used a rectenna array and efficiency of 20% was achieved for power density 62 μW/cm^2 or equivalently for power input 13.27 dBm (for rectenna geometric area of 342.25 cm^2). In [7], maximum efficiency of 77.8% was achieved for 10 dBm input. In [8], efficiency of 54% was obtained for power density 200 μW/cm^2 or for 9.54 dBm power input (assuming rectenna geometric area of 45 cm^2). Finally, rectenna in [9] was designed with analytical models and closed-form expressions, with obtained efficiency of 40% for 0 dBm.

Considerable research effort has been also made towards high-efficiency rectennas for *low* power input, e.g. less than 0 dBm [10]–[22]. In [10], authors harvested energy from a TV station tower 6.3 km away and maximum efficiency of 21% was achieved for −4.74 dBm power input. A multi-band harvesting system was presented in [11]; a single wide-band antenna was connected to multiple narrow-band rectifier paths. The rectifier outputs were joined together adding the dc voltages and the maximum obtained efficiency was approximately 27% for −10 dBm power input. In order to further increase the efficiency, substrates with low losses [12]–[15] have been proposed, increasing however the total cost. In [12], a multi-band rectenna was used, operating at 900 MHz and 1750 MHz, with measured efficiency of 44.5% and 34.5%, for power input −8.77 dBm and −16.27 dBm, respectively. In [13], the rectenna operated at 900 MHz with 33% efficiency for −10 dBm input power. In [14] efficiency was increased to 50% for −17.2 dBm at 2.4 GHz. A circular polarized rectenna was presented in [15] with 15.3% and 11.3% efficiency for vertical and horizontal polarization, respectively. In [16], authors proposed a hybrid harvesting system consisting of both a rectenna and a solar panel. The rectenna was dual-band (850 MHz, 1850 MHz) with 15% efficiency at both frequency bands, for −20 dBm power input.

In [17], [18], emphasis was on the required impedance matching circuit inductances, while minimizing the reflection coefficient, with attained efficiency of 17% and 20.5%, respectively, for −20 dBm power input. However, single (and not double) rectification was exploited, while the optimization process did not have load or rectenna microstrip dimensions as optimization degrees of freedom (as in this work), while cost function included reflection coefficient only and excluded efficiency (as opposed to this work). Furthermore, [17] used no boost converter and no rectenna array, while work in [18] utilized a custom boost converter and added the rectenna array currents (and not voltages, as in this work). In [19], energy was harvested from a digital TV station with efficiency of 18.2% for −20 dBm. In [20], ambient RF power was collected

TABLE I
RF-TO-DC CONVERSION EFFICIENCY VS POWER INPUT/DENSITY & FREQUENCY.

work	efficiency	power input (dBm)	frequency (MHz)
[5]	65%	25	2450
[6]*	20%	13.27	2000 − 18000
[7]	77.8%	10	2400
[8]**	54%	9.54	1960
[9]	40%	0	2450
[10]	21%	−4.74	512 − 566
[11]	27%, 25%	−10, −10	539, 915
[12]	44.5%, 34.5%	−8.77, −16.27	900, 1750
[13]	33%	−10	900
[14]	50%	−17.2	2450
[15]	15.3%	−20	2450
[16]	15%	−20	850, 1850
[17]	17%	−20	868
[18]	20.5%	−20	868
[19]	18.1%	−20	470 − 770
[20]***	40%	−25.4	2110 − 2170

*$A = 18.5 \times 18.5$ cm^2, $S = 62$ μW/cm^2.

**$A = 7.5 \times 6$ cm^2, $S = 200$ μW/cm^2.

***The end-to-end efficiency of one charge–discharge operation cycle, without considering startup.

and the end-to-end (rectenna and boost converter) efficiency was estimated in normal operation, without considering the startup time (i.e. the time needed to start charging from 0 V). Furthermore, the harvesting system in [21] operated at −20 dBm RF input power and stored 5.8 μJ into a rechargeable battery within 1 hour, while sub-micron CMOS technology was used in [22] and the harvesting system supplied a wireless sensor node from −19.7 dBm power input. Table I offers summary of achieved efficiency versus input power (or power density) and frequency, for various prior art designs.

Another critical parameter in RF energy harvesting is the rectenna dc output voltage. A typical rectenna is designed to supply with energy small electrical devices, which usually operate only above a cut-off voltage level. Hence, the rectenna output voltage should support such design requirement. In RF-to-dc rectification, the number of diodes - or equivalently the number of voltage multiplier stages - affects the rectifier efficiency and the rectified dc output voltage [23]; for low power input, when the number of diodes is decreased, efficiency will be increased and output voltage will be decreased; when the number of diodes is increased, the opposite happens. Therefore, in order to increase voltage, authors in [10] used a 5-stage Dickson RF-to-dc voltage multiplier. The output voltage across a 1 MΩ load was 5 V for −4.74 dBm power input, while the efficiency was 21%. In [11], authors proposed a hybrid multi-stage and multi-band RF harvesting system with one directional, log-periodic, wide-band antenna. For power input −10 dBm, the maximum efficiency was 27% and was decreased to 20% when the number of frequency bands where RF harvesting takes place, or equivalently the number of diodes, was increased from 2 to 5. Moreover, the output

voltage across a 100 kΩ load was 2.3 V and 2.5 V, when power input was −12.76 dBm and −12.04 dBm, respectively.

In order to overcome the problem of multiple diodes, two other solutions have been proposed. The first is the multiple branches approach [13]; one branch is used for the start-up stage and the other for the boost converter, with achieved output voltage of 2 V for −15.5 dBm power input. The second solution is a rectenna-area design in which multiple rectennas are combined at the dc area, while operating at the same or different frequency band. In [20], authors tested two configurations: a) multiple rectennas, which harvest energy from different frequency bands, sharing one boost converter, with obtained end-to-end efficiency of 15%; b) multiple rectennas, sharing multiple boost converters, with obtained end-to-end efficiency of 13%. At both cases, RF input power was −12 dBm.[1] The output voltage from the rectenna array at both cases was over 330 mV, which was adequate to start the boost converter. The latter's open-circuit output voltage reached 2.84 V. In [18], authors used a 1×2 rectenna array with rectennas operating at the same frequency. The rectenna array output voltage across a 5 kΩ load was 110 mV for −20 dBm power input. Next the load was removed and the rectenna was connected to a boost converter; the open-circuit voltage at the output of the rectenna array and the boost converter was 298 mV and 1.4 V, respectively.

Given the non-linear output impedance of rectennas and their variable efficiency at different input power density levels, it has become apparent that power management circuitry designs should be carefully designed; work in [24] designed a power management circuit between rectenna and energy storage, with discrete components, for maximum power point tracking and operation as low as 10 − 100 μW, targeting RF harvesting from cellular base stations; the latter offer energy that can easily vary by two orders of magnitude, within 24h of operation. For input power below 100 μW, losses of quiescent operation become challenging. Work in [25] presents a custom power management integrated circuit (IC) with resistor emulation technique, which can operate at low power on the order of 1 μW, requiring however external power at start-up, in addition to the RF-harvested power. Work in [26] discussed joint designs of rectenna and power conversion management in order to supply a wireless transceiver using power management circuitry principles as in [24], [25] and power input densities as low as 1.74 μW/cm^2 (corresponding to −12 dBm for a 6×6 cm^2 patch antenna), while work in [27] offered designs for input power densities as low as 0.62 μW/cm^2, exploiting power management circuitry, rectenna arrays in various connection configurations and large antenna gain for the startup circuit.

This work operates a scatter radio duty-cycle sensor with input power level densities as low as 0.0139 − 0.1 μW/cm^2, using careful rectenna design methodology and certain modifications on a commercial power management boost converter. Specifically, the goal of this work was to:

1) design an efficient and sensitive rectification system (i.e.

---

[1]It is noted that the presented efficiency for [20] on Table I refers to the maximum end-to-end efficiency for only one rectenna (not rectenna array).

operation at low power input), e.g. around or below -20 dBm,

2) maximize the rectified dc output voltage,
3) offer a complete supply solution for scatter radio, duty-cycle WSN nodes with RF harvesting, without any utilization of additional external power (e.g. for starting the boost converter).

In sharp contrast to prior art designs, it was shown that minimization of the reflection coefficient only was not sufficient for maximization of the RF-to-dc efficiency. Specifically, in contrast to prior art (e.g. [17], [18]) the design procedure of this work formulated a multi-objective optimization problem with two goals, i.e. minimization of reflection coefficient and maximization of RF-to-dc efficiency. Moreover, it was shown that *all* rectifier trace dimensions (e.g. the distance between diode and load) and not only the matching network trace dimensions and lumped elements (e.g. inductances), affect the RF-to-dc efficiency. Hence, during the rectifier design/optimization,

- the optimization variables, i.e. the *degrees of freedom* were not only the matching network parameters but also all other trace dimensions (e.g. the distance between diode and load, the diode and the port input),
- load was also a degree of freedom,
- minimum reflection coefficient *and* maximum RF-to-dc efficiency were simultaneously targeted.

Based on this design procedure, the proposed harvesting system is both analytically and experimentally shown to offer high efficiency and high sensitivity (i.e. it can operate at low input power density).

Furthermore, in contrast to prior designs, the proposed harvesting system can supply continuously, *without* a boost converter or use of any energy tank (e.g. big capacitor), at low input power density of 0.1103 $\mu\mathrm{W/cm^2}$, a battery less backscatter sensor node, which consumes power on the order of 100 μW and operates with voltage greater than 1.6 V. Moreover, whenever a boost converter was needed (e.g. for extra low power density, below 0.1 $\mu\mathrm{W/cm^2}$), the latter was self-started, using the designs of this work, without utilization of any additional external power source. The proposed harvesting system, is not only of high sensitivity, but also of high efficiency, compared to state-of-the-art: for low-power input, e.g. for -20 dBm, rectifier offers 28.4% RF-to-dc efficiency, while for -10 dBm the efficiency is 43.77%.

This paper is organized as follows. The rectifier is presented in Section II, with description of geometry, design/optimization procedure, reflection coefficient and RF-to-dc efficiency, including measurements. Section III presents the design of the rectenna, including measurements of RF-to-dc efficiency. Multiple rectennas are also combined, forming rectenna arrays and the open-circuit voltage is measured for various input power levels. Section IV presents the end-to-end RF harvesting supply system for a custom scatter radio, duty-cycle WSN node. Finally, Section V concludes this work.

II. RECTIFIER

A single series circuit with a double diode was designed, analyzed, optimized and fabricated. The obtained rectifier
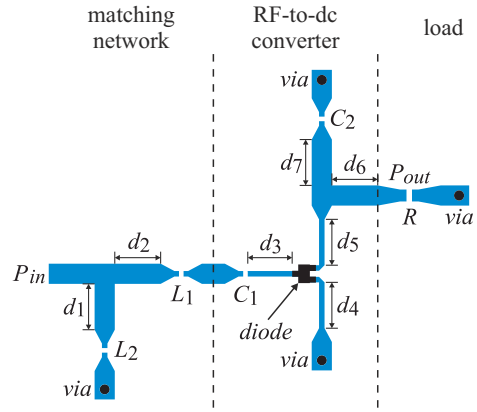

Fig. 1. The microstrip rectifier design (top layer).

TABLE II
OPTIMIZED TRACE DIMENSIONS (mm).

d_1	d_2	d_3	d_4	d_5	d_6	d_7
1.5350	5.6001	6.1796	7.6296	0.5003	4.4366	3.2024

offers high efficiency (i.e. greater than 28%) for low power input (i.e. bellow -20 dBm) or equivalently for low power density (i.e. bellow 0.07 $\mu\mathrm{W/cm^2}$), low-complexity and low-cost. The latter was achieved using the widely used but lossy FR-4 substrate, despite the fact that losses decrease efficiency. In order to increase efficiency, emphasis was given on the optimization process, as explained bellow.

The whole geometry is depicted in Fig. 1. The RF power input is converted to dc power through the low-cost Schottky double diode "HSMS285C". The matching circuit reduces the reflection losses of the incoming wave, while the capacitors C_1, C_2 were introduced in order to stabilize the obtained dc voltage. Finally, the output power supplies load R.

A. Analysis and Optimization

The rectifier was designed to operate at 868 MHz, taking into account the UHF RFID frequencies in Europe. Initially, full electromagnetic analysis with the method of moments was applied to the microstrip trace only, in order to estimate the losses from the low-cost FR-4 and copper, the fringing fields and the electromagnetic coupling between ports. The FR-4 was modeled with $\epsilon_\mathrm{r} = 4.55$, $\tan\delta = 0.01$, copper thickness 35 μm and substrate height 1.5 mm. Next, harmonic-balance and large-signal analysis was employed, taking into account the non-linear behavior of the rectifier due to the diode. In this work a new design procedure is proposed in order to enhance the rectifier efficiency and sensitivity, for low power input.

Firstly, the goal was not only the minimization of reflection coefficient,

$$\Gamma = \frac{Z_\mathrm{in} - 50}{Z_\mathrm{in} + 50}, \tag{1}$$

at the rectifier input port (assuming antenna impedance of 50 Ω), but also the maximization of the RF-to-dc efficiency,

$$\eta = \frac{P_\mathrm{out}}{P_\mathrm{in}} = \frac{V_\mathrm{R}^2/R}{P_\mathrm{in}}, \tag{2}$$
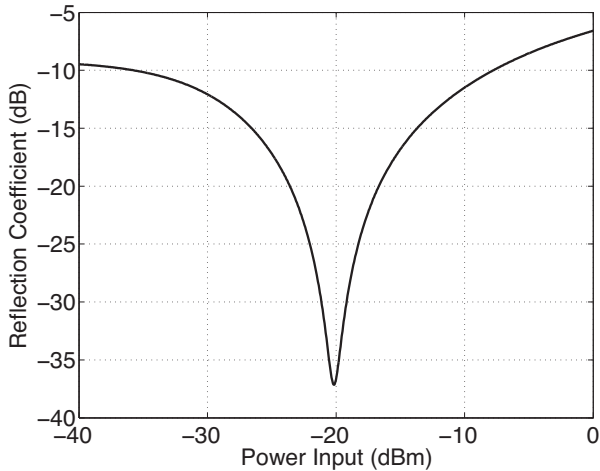
Fig. 2. Simulated reflection coefficient, S_{11}, at 868 MHz versus power input. The rectifier operates from -35.7 to -7.8 dBm.
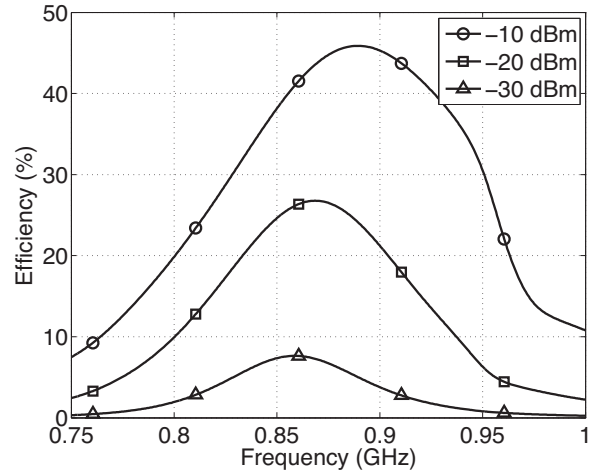

Fig. 4. Simulated rectifier efficiency versus frequency for different power input levels. Load is fixed at 9530 Ω.
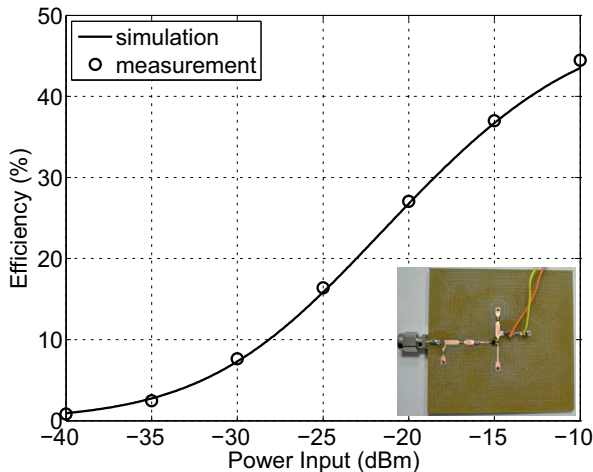

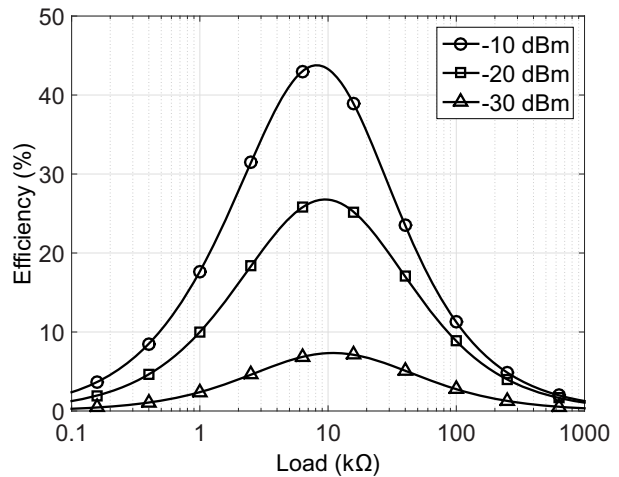Fig. 3. Simulated and measured rectifier efficiency versus power input at 868 MHz.

Fig. 5. Simulated rectifier efficiency versus load for different power input levels at 868 MHz.

with P_{in} and P_{out} the power input and output, respectively and V_{R} the voltage across R.

Secondly, the optimization degrees of freedom were not only the matching network microstrip dimensions (d_1, d_2 and lumped elements, L_1, L_2 in Fig. 1), but also the microstrip dimensions of the *whole* rectifier, including distance:

- d_3 between the diode and capacitor C_1,
- d_4 between the diode and via,
- d_5 as shown in Fig. 1,
- d_6 between the diode and the load,
- d_7 between the diode and capacitor C_2.

Thirdly, the load R was also a design parameter. It is noted that dimensions parameters d_i, $i = 1, 2, ..., 7$ can take continuous values, while L_1, L_2 and R can take only discrete values. On the other hand, the capacitances C_1, C_2, the power input P_{in} and the frequency were fixed at 100 pF,

-20 dBm and 868 MHz, respectively.[2] Hence, in contrast to prior art (e.g. [17], [18]), the design procedure is a multi-objective optimization problem (i.e. two simultaneous goals) with multiple (i.e. ten) degrees of freedom. Finally, a genetic algorithm was applied to solve this optimization problem.

After such optimization methodology (denoted as "optimization no. 1"), the obtained lumped elements were $L_1 = 12$ nH, $L_2 = 1.2$ nH and $R = 9530$ Ω, while the optimized trace dimensions are tabulated on Table II. The simulated Γ is depicted in Fig. 2. It is shown that the rectifier's reflection coefficient is bellow -10 dB for P_{in} between -35.7 and -7.8 dBm, i.e. for low-power input. Fig. 3 depicts η versus P_{in}. According to simulated results, the efficiency is equal to 43.5% and 7.31% for P_{in} equal to -10 dBm and -30 dBm, respectively, and 26.77% for $P_{\text{in}} = -20$ dBm. It is known that the efficiency is a function of frequency, as well as load and

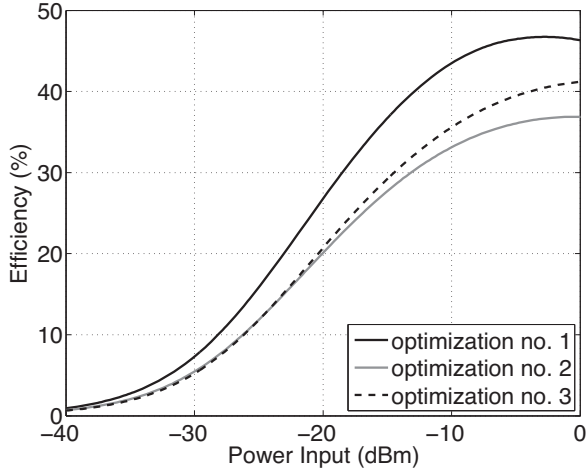[2]Operational bandwidth in the UHF 900 MHz regime is also examined subsequently.

Fig. 6. Simulated RF-to-dc efficiency versus input power for various optimization/design procedures.

power input, due to the diode non-linearity. Such non-linear relation is examined subsequently.

The simulated efficiency versus frequency for various power input levels and load fixed at 9530 Ω, is depicted in Fig. 4. It is shown that the rectifier operates optimally at 868 MHz for $P_{\text{in}} = -20$ dBm, as expected. For -10 dBm input power, the maximum efficiency of 45.9% is achieved at 889 MHz, while for $P_{\text{in}} = -30$ dBm, maximum efficiency of 7.4% is found at 858.5 MHz. Fig. 5 depicts the relation between the efficiency and the load for various power input levels, with the frequency fixed at this time at 868 MHz. For $P_{in} = -20$ dBm, maximum $\eta = 26.77\%$ occurs when $R = 9530\ \Omega$, as expected due to the optimization process. For $P_{\text{in}} = -10$ dBm and $P_{\text{in}} = -30$ dBm, maximum efficiency is equal to 43.77% and 7.34% for 8.17 kΩ and 10.96 kΩ load, respectively. Both efficiencies are close to the respective ones for $R = 9530\ \Omega$ (the latter is the selected value for -20 dB).

In order to show that microstrip trace dimensions affect the efficiency and minimization of reflection coefficient only does not guarantee RF-to-dc efficiency maximization, two additional rectifiers were designed. In "optimization no. 2", parameters to be optimized were matching network inductance (L_1, L_2) and load (R), while minimizing reflection coefficient only. In "optimization no. 3", optimization parameters were again matching network inductance (L_1, L_2) and load (R), while minimizing reflection coefficient *and* maximizing efficiency, simultaneously. Other parameters were fixed: $d_{\text{i}} = 3$ mm, where i $= 1, 2, ..., 7$ and $C_1 = C_2 = 100$ pF. Fig. 6 depicts the resulted efficiency. It is evident that the maximum RF-to-dc efficiency took place only when the approach of this work ("optimization no. 1") was applied. The latter can be explained as follows: reflection coefficient quantity shows the amount of reflected power due to the impedance mismatch between the source and the rectifier. Minimizing reflection coefficient leads to maximizing the rectifiers power input, but does not guarantee that the whole amount of this power will be transformed to dc power (e.g. minimization of reflection coefficient does not take into account losses on substrate).

On the other hand, efficiency shows the rectifier's ability to convert the input RF power to dc power, and hence, it takes into account possible losses (e.g. substrate and diode losses).

B. Measurements

The rectifier was fabricated with a CNC milling method (Fig. 3, inset). A signal generator was connected to the rectifier. The frequency was fixed at 868 MHz and the power input was varied from -40 dBm to -10 dBm; load R was fixed at 9530 Ω and the voltage across R was measured. The RF-to-dc efficiency was estimated via (2) and the measured results are depicted in Fig. 3. Agreement between simulations and measurement can be observed; for $P_{\text{in}} = -20$ dBm, the measured efficiency is 27.1%, while for $P_{\text{in}} = -10$ dBm and $P_{\text{in}} = -30$ dBm, $\eta = 44.5\%$ and $\eta = 7.65\%$, respectively.

III. RECTENNA

Initially, a monopole antenna was designed, analyzed, fabricated and finally merged with the rectifier, forming a rectenna. The latter's efficiency was measured with a specific methodology explained below.

A critical rectenna parameter, except from the RF-to-dc efficiency, is the offered power to the load and the rectenna dc output voltage, as already mentioned. The latter requirement is obtained from the fact that usually the rectifier is connected to a dc-to-dc boost converter, which only operates above a cut-off voltage and current level. On the other hand, ambient power density is usually below 1 μW/cm^2 [10], [19], [20]. Hence, it is an engineering challenge to harvest as much power as possible and increase the rectenna dc output voltage for low power density. Prior art has used multi-band rectennas with multiple diodes [10], [11], multiple branches [13], rectenna arrays operating on same [6] or different [20] frequency bands in order to increase the rectified dc-power and output voltage. However, most of these designs operate optimally for power input greater than -12 dBm.

In this work, the goal was to implement a harvesting system for low power input and power density, less that -20 dBm and 0.07 μW/cm^2, respectively. Hence, a rectenna and rectenna array topology was implemented and tested in terms of radiation pattern, efficiency, output power and open-circuit voltage. The ability of one rectenna or rectenna array scheme, combined with a commercial dc-to-dc converter, to provide energy to a backscatter sensor node for low-power density was also examined.

A. Antenna

A microstrip monopole antenna was merged with the proposed microstrip rectifier, in order to obtain a plane rectenna. Specifically, a hybrid microstrip monopole bow-tie-inspired antenna was designed to operate at RFID band in Europe (around 868 MHz). The two arms of a conventional bow-tie were placed on different sides of FR-4 substrate, in a symmetric manner. A copper trace was connected with one of the two arms, forming a feeding microstrip line with the other arm. The obtained antenna was first simulated and then fabricated.
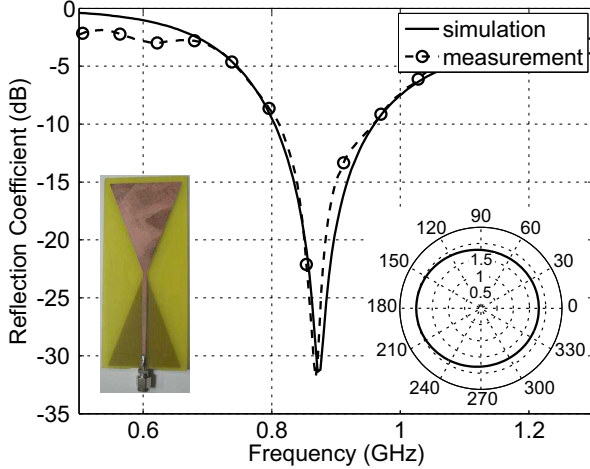
Fig. 7. Bow-tie-inspired monopole antenna reflection coefficient and radiation pattern (inset, right) at horizontal plane ($\theta = 90°$) in terms of realized gain (in dB). The fabricated antenna is also shown (inset, left).

Fig. 8. Antenna to rectifier matching bandwidth for different power input levels.

Good agreement between simulation and measurement results is shown in Fig. 7.

The latter also shows the antenna gain at horizontal plane; gain G is equal to 1.7 dB and 2 dB at $\phi = 0°$ and $\phi = 180°$, respectively, and $G = 1.8$ dB for $\phi = \pm 90°$; thus, the antenna is appropriate for ambient power harvesting due to its almost omni-directional radiation pattern.[3]

B. Rectenna Performance

In this section the hybrid bow-tie-inspired monopole was connected to the rectifier, forming the rectenna. The latter's operation bandwidth depends on input power and load. Assuming that Z_a and Z_r is the antenna and rectifier input impedance, respectively, the rectenna operational bandwidth (i.e. matching bandwidth) is defined where:

$$|\Gamma_r| = \left| \frac{Z_r - Z_a^*}{Z_r + Z_a} \right| < -10 \text{ dB}, \qquad (3)$$

where, $\{*\}$ denotes the conjugate of Z_a. Fig. 8 shows the matching bandwidths for various input power levels at fixed load of 9530 Ohm. For -10, -20, and -30 dBm input power, the rectenna operates within $862.8 - 939.3$, $842.2 - 912.1$ and $844.1 - 881.4$ MHz, respectively. Hence, the proposed rectenna can capture and convert RF to dc power not only at 868 MHz but also within GSM 850 and GSM 900 cellular bands. Nevertheless, the rectenna was tested for a single frequency, i.e. at 868 MHz only, for a fair comparison with prior art designs.

The proposed rectenna RF-to-dc efficiency was estimated with the measurement topology of Fig. 9. Initially, a signal generator was placed at "point a", transmitting at different power levels with a log-periodic antenna at 868 MHz ("phase 1"). A calibrated antenna was placed at far-field distance, at "point b" (a commercial monopole with gain $G_{cal} = 1.8$ dB).

[3]The radiation pattern is not perfectly omni-directional due to fabrication defects.

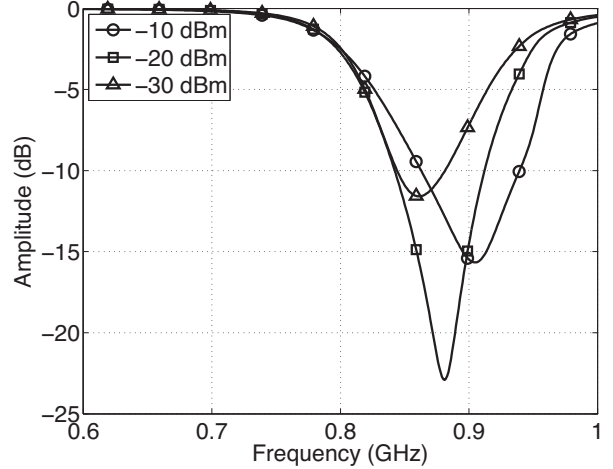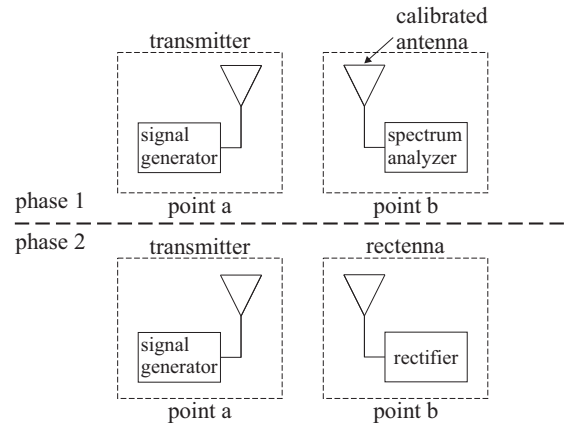Fig. 9. The rectenna RF-to-dc efficiency measurement two-phase methodology.

The monopole was connected to a spectrum analyzer and received power P_{cal} was measured. Next, the calibrated antenna and the spectrum analyzer were removed, the proposed rectenna was placed at exactly the same location ("point b") and voltage across load V_R was measured ("phase 2").

The rectenna RF-to-dc efficiency is estimated by:

$$\eta = \frac{P_{out}}{P_{in}} = \frac{V_R^2/R}{S \cdot A_{eff}}, \qquad (4)$$

where S is the power density of the incident to the rectenna plane wave and A_{eff} the total antenna effective area given by:

$$A_{eff} = \frac{\lambda^2}{4\pi} G, \qquad (5)$$

where λ is wavelength at 868 MHz and G is the rectenna gain. The rectenna was placed in parallel to the transmitter and thus, $G = 1.8$ dB according to Fig. 7, inset. Hence from (5) $A_{eff} = 143.67$ cm^2. The power density is calculated by:

$$S = \frac{4\pi}{\lambda^2} \frac{P_{cal}}{G_{cal}}, \qquad (6)$$

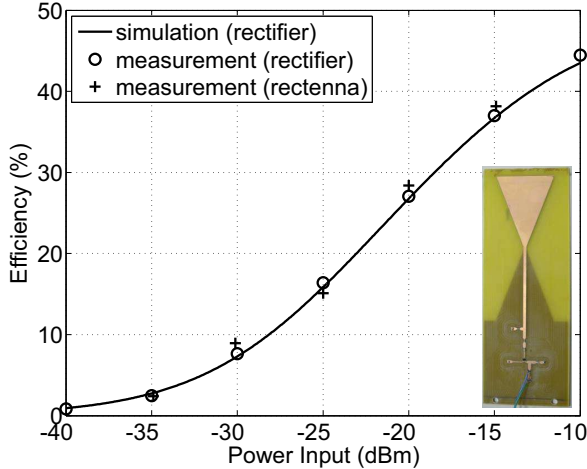after measuring P_{cal} and using $G_{cal} = 1.8$ dB (i.e. the gain of the commercial monopole).

Fig. 10. Measured rectenna efficiency versus power input. Measurement and simulation results of the rectifier are also depicted. Inset: the fabricated rectenna.

Fig. 11. Measured rectenna output voltage across the 9530 Ω load.

The measured RF-to-dc efficiency is calculated from (4)-(6) and it is shown in Fig. 10. Measured rectifier efficiency (without antenna in Fig. 3) and rectifier simulation results are also depicted. Good agreement can be observed. Specifically, for $P_{\text{in}} = -20$ dBm, $\eta = 28.4\%$, while for -30 dBm and -10 dBm, η is 9% and 44.2%, respectively. Fig. 11 shows the measured voltage values across the 9530 Ω load. It can be observed that $V_{\text{R}} = 164.5$ mV for $P_{\text{in}} = -20$ dBm, while for -30 dBm and -10 dBm the voltage is 29.3 mV and 649 mV, respectively.

The measured and simulated rectenna efficiency versus power density are depicted in Fig. 12, showing again good agreement. For $S = 1$ $\mu\text{W/cm}^2$ the efficiency is 44.8%, while for 0.1 $\mu\text{W/cm}^2$ and 0.01 $\mu\text{W/cm}^2$, η is 30.2% and 9.57%, respectively. It is noted that for $S = 0.0696$ $\mu\text{W/cm}^2$ and rectenna gain $G = 1.8$ dB, according to (4), (5) $P_{\text{in}} = -20$ dBm and $\eta = 28.4\%$.

C. Rectenna Array

The input power in a rectifier system is proportional to the rectenna effective area or equivalently to the rectenna gain. Hence, according to Eq. (4), in a rectifier system with given efficiency, the offered power to the load will be increased if the rectenna gain is increased (although such increment does not guarantee that dc output voltage will be also increased). On the other hand, antenna gain increase could potentially lead to complex rentenna designs with directional radiation pattern, which may not be desirable for ambient harvesting. Another approach increases the number of rectennas, where each rectenna is considered as a dc voltage source. The latter approach was used in this work.

Two rectenna array topologies with two alignments were tested, depicted in Fig. 13: antennas were placed alongside the x-axis ("horizontal"-alignment) or alongside z-axis ("vertical"-alignment). At both alignments, rectenna plane was parallel to yz-plane.

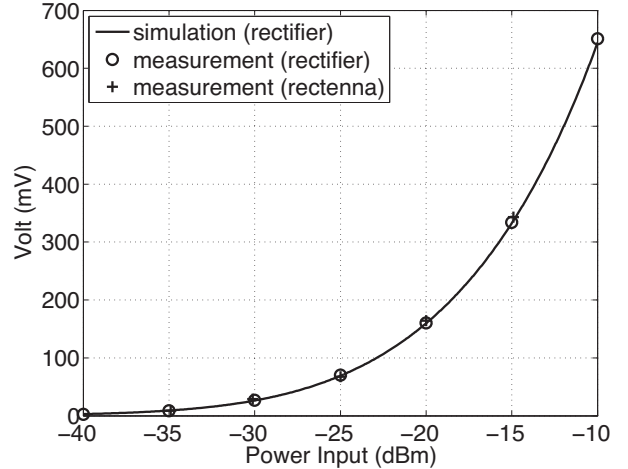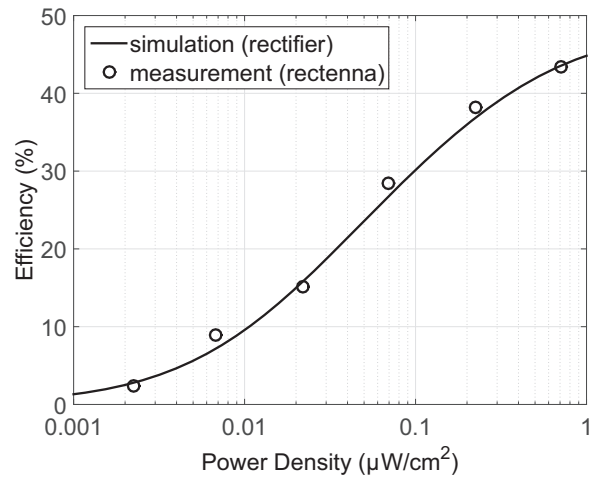Fig. 12. Measured rectenna efficiency versus ambient power density.

Due to the rectennas proximity, the rectenna array radiation pattern should be estimated. Rectennas were placed at $\lambda/2$ or equivalently $d = 17.5$ cm (Fig. 13) in order to maximize gain [28] and keep mutual coupling between rectennas at low level, i.e. less than -10 dB. The whole geometry was analyzed at 868 MHz, with one antenna radiating and the other/others (with the rectifier/rectifiers) acting as parasitic elements. The final radiation pattern resulted from the combination of the constituting individual rectennas. Fig. 14 depicts the gain (in dB) for "horizontal" and "vertical" -alignment for 1×2 and 1×3 rectenna array. In "horizontal"-alignment the maximum gain was 4.67 dB and 6.43 dB for 1×2 and 1×3, respectively, and $\theta = 90°$ (i.e. at horizontal plane) and $\phi = \pm 90°$. Radiation pattern was omni-directional for "vertical"-alignment; the gain was 4.36 dB and 6.1 dB for 1×2 and 1×3 rectenna array, respectively. At all cases, reflection coefficient and mutual coupling was less than -18 dB.

Rectennas were electrically connected in series configuration (voltage summing) in order to increase the offered to the load power and the output voltage. The obtained rectenna ar-
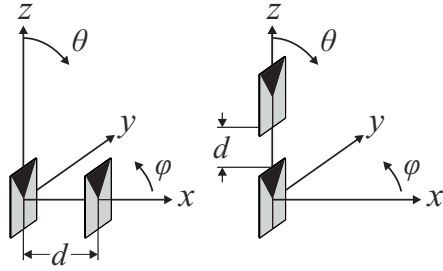
Fig. 13. 1×2 rectenna array topology: "horizontal" (left) and "vertical" (right) -alignment. 1×3 topology was also tested.
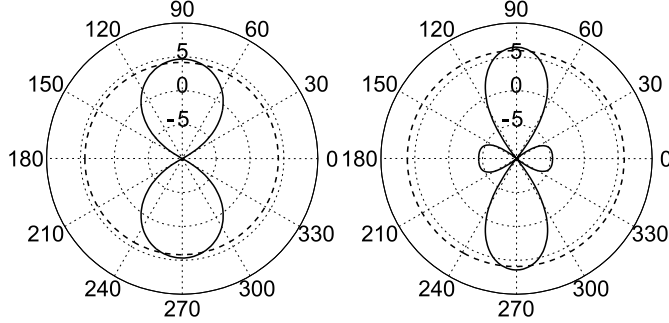

Fig. 14. The radiation pattern at horizontal plane ($\theta = 90°$) in terms of gain (in dB) for 1×2 (left) and 1×3 (right) rectenna array, at "horizontal" (solid-line) and "vertical" (dashed-line) -alignment.

rays were placed at far-field distance from a transmitter and the dc open-circuit voltage was measured. The efficiency measurement procedure was similar to that followed for one rectenna. Fig. 15 (inset) illustrates the measurement setup; a signal generator with one log-periodic antenna was the transmitter. The rectenna array at "horizontal"-alignment was placed at far-field distance and the open-circuit voltage was measured through a voltmeter. The power density, which was dependent on the transmitted power, varied from 0.01 μW/cm^2 to 1 μW/cm^2. The measurement results are depicted in Fig. 15. It is observed that as the number of the rectennas increases, the dc voltage is also increased. The open-circuit voltage was 0.515 V, 1.15 V and 1.97 V when one, two and three rectennas harvest energy for $S = 0.1$ μW/cm^2, respectively.

Fig. 16 depicts the open circuit voltage versus the number of rectennas placed at "horizontal"-alignment for 0.1 μW/cm^2 power density. It is evident that voltage is the linear addition of each rectenna, or equivalently, rectenna addition offers close to addition of rectified signals. Additional theoretical work is further needed, left for future work.

IV. SUPPLYING A BACKSCATTER SENSOR NETWORK NODE

This section studies the ability of the proposed rectenna to supply with power a duty-cycle backscatter sensor node for low-power density. Again, a log-periodic antenna, connected to a signal generator, transmits power at 868 MHz. A rectenna-scheme, placed at the far-field, harvests and converts RF energy to dc voltage. The rectenna array output is connected to the backscatter sensor node presented in [3], which consumes power on the order of 100 μW and operates with voltage greater than 1.6 V.
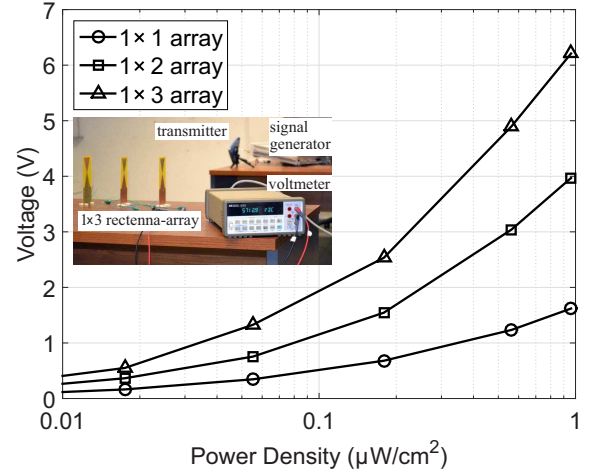

Fig. 15. The measured open-circuit voltage versus power density for one, two or three rectennas at "horizontal" alignment.
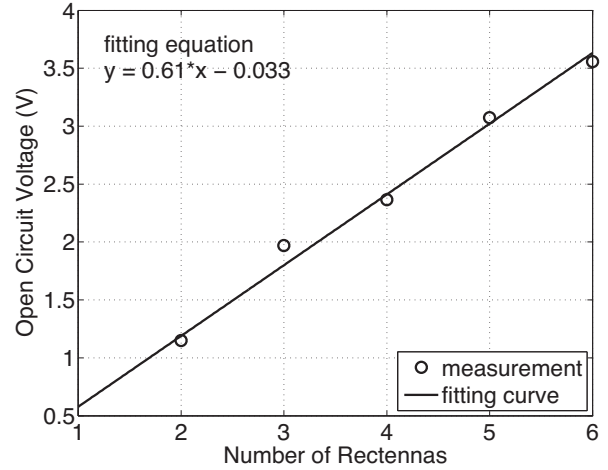

Fig. 16. The measured open-circuit voltage versus number of rectennas at "horizontal" alignment for 0.1 μW/cm^2 power density.

According to Fig. 15, when 1×3 rectenna array is used, the open-circuit voltage is greater than 1.9 V for S over than 0.1 μW/cm^2. Hence, it is possible to directly and continuously supply with energy the backscatter sensor node [3] without use of any boost converter. Thus, the 1×3 rectenna array was placed at far-field in "horizontal"-alignment. Rectennas were connected in series configuration and the output was directly connected to the sensor node. More specifically, the power density was 0.1103 μW/cm^2 or equivalently $P_{cal} = -18$ dBm, given $G_{cal} = 1.8$ dB and $P_{in} = -13.37$ dBm, according to Eq. (7). Input voltage to sensor was 1.69 V, while the open-circuit voltage was about 2 V (Fig. 15). In order to validate the backscatter operation of the sensor node, a conventional monopole antenna was connected to a spectrum analyzer and the received spectrum band depicted the obtained peak at frequency F_c and the subcarrier peaks at $F_c \pm F_0$, due to sensor switching its antenna between two states at frequency F_0.
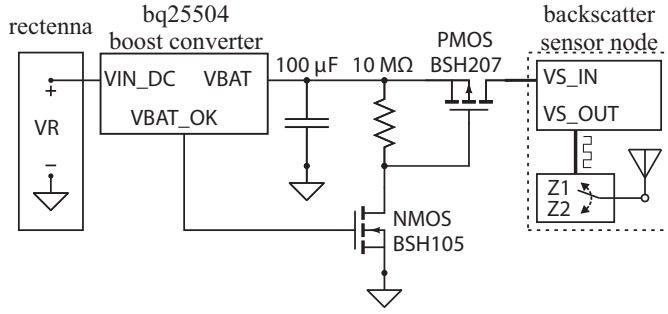
Fig. 17. Boost converter schematic with the low-power "bq25504".

Fig. 18. Measurement setup with DAQ instrument.

According to Fig. 15, only one rectenna offers open-circuit voltage greater than 1.6 V, when S is greater than 0.9346 μW/cm^2. Similarly, for 1×2 and 1×3 rectenna array, voltage is greater than 1.6 V when S is greater than 0.1866 μW/cm^2 and 0.0721 μW/cm^2, respectively. Hence, a boost converter is needed for the sensor of [3], when S is less than 0.1 μW/cm^2 and one or two rectennas are used.

In this work, the low-power boost converter "bq25504" was utilized [29]. The latter is an integrated-circuit with maximum power point tracking (MPPT), minimum cold start voltage and typical input power of 330 mV and 10 μW, respectively, and low quiescent current ($\leq$ 330 nA). Hence, for minimum voltage of 330 mV and typical power of 10 μW, the boost converter input impedance is 10890 Ohm, which is close to 9530 Ohm (i.e. the load value for optimum RF-to-dc efficiency of the proposed rectenna). However, due to the MPPT function (which aims to extract the maximum power from the rectenna output), as well as the fact that the boost converter has two main operational modes (one for cold-start operation and one after cold-start, with main boost charger enabled), the input impedance does not remain constant. The MPPT functionality includes periodic sampling of the input (open) voltage signal, after disabling the charger for a limited duration of time (on the order of 256 ms every 16 sec); the cold start charger is an unregulated, hysteretic boost converter with lower efficiency compared to the main boost charger and provides the initial power so that the latter can start its operation. This work measured experimentally the end-to-end input-output relationship of the whole system, as described below.

Initially, only one rectenna was connected to the analog backscatter sensor node through the "bq25504". Fig. 17 depicts the circuit schematic topology. Rectenna voltage ($V_R \equiv V_{IN\_DC}$) was boosted (V_{BAT}) and a 100 μF capacitor was charged from 0 V. It is noted that the boost converter was self-started (cold start) and no external energy was used. Digital signal output (V_{BAT_OK}) is set to high and low, when the capacitor voltage reaches a pre-defined upper and lower limit, respectively. In this work, the boost converter was designed to have low and upper voltage threshold 2.4 V and 2.8 V, respectively.

An external PMOS ("BSH207") was placed between the sensor node and the V_{BAT} pin. The inverted V_{BAT_OK} signal (through the open drain NMOS "BSH105") was used to drive the gate of t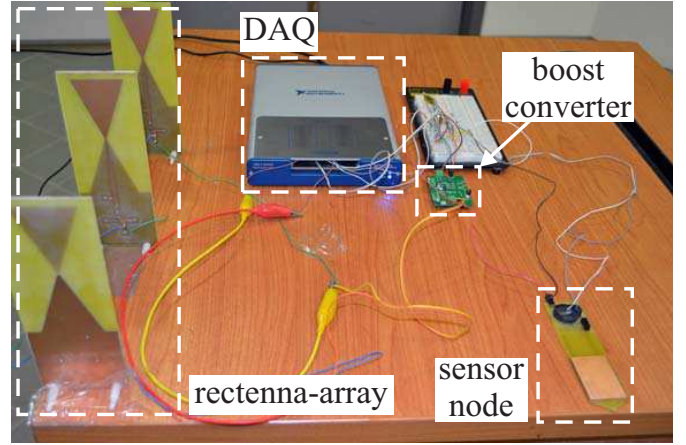he PMOS. While V_{BAT} is lower than 2.8 V, PMOS stays off (zero current) and the boost converter charges the capacitor. Next, when the V_{BAT} reaches 2.8 V, PMOS turns on and energy flows from the capacitor to the sensor. The latter operates and voltage squared pulses (V_{S_OUT}) are produced that control the backscatter RF transistor of the sensor [3]. Next, capacitor is discharged and when $V_{BAT} = 2.4$ V, PMOS turns off again and current stops flowing to the sensor. Then, the capacitor is charged again until $V_{BAT} = 2.8$ V and the procedure is repeated. A data acquisition (DAQ NI USB-6356) instrument was used in order to measure the voltage across the rectenna output (V_{IN_DC}) and the capacitor (V_{BAT}). The measurement setup is depicted in Fig. 18.

Fig. 19(a) illustrates the measurement voltages for one rectenna at $S = 0.1103$ μW/cm^2. This power density corresponds to $P_{cal} = P_{in} = -18$ dBm, given $G_{cal} = G = 1.8$ dB. It is observed that the 100 μF capacitor needs 530 s to be charged from 0 V (cold start) to 2.8 V. Then, the sensor node, operates every 25 s. For less power density, i.e. $S = 0.0876$ μW/cm^2, or equivalently for $P_{cal} = P_{in} = -19$ dBm the capacitor is charged after 1498 s and sensor operates every 44 s (Fig. 19(b)).

Next, two rectennas were connected in series configuration at the dc-area, according to "horizontal"-alignment. The obtained 1×2 rectenna array was connected to the sensor node through the "bq25504" boost converter. Power density was 0.0439 μW/cm^2, corresponding to $P_{cal} = -22$ dBm, given $G_{cal} = 1.8$ dB. From (5)-(6),

$$P_{in} = \frac{G}{G_{cal}} P_{cal}. \qquad (7)$$

According to Fig. 14, $G = 4.67$ dB in this case, hence $P_{in} = -19.13$ dBm. The first time charging duration and the operating period were 938 s and 30 s, respectively (Fig. 19(c)). Then, power density was further decreased to 0.0220 μW/cm^2 or equivalently, $P_{cal} = -25$ dBm and $P_{in} = -22.13$ dBm. Capacitor was charged after 1655 s and the sensor node operated every 49 s (Fig. 19(d)).
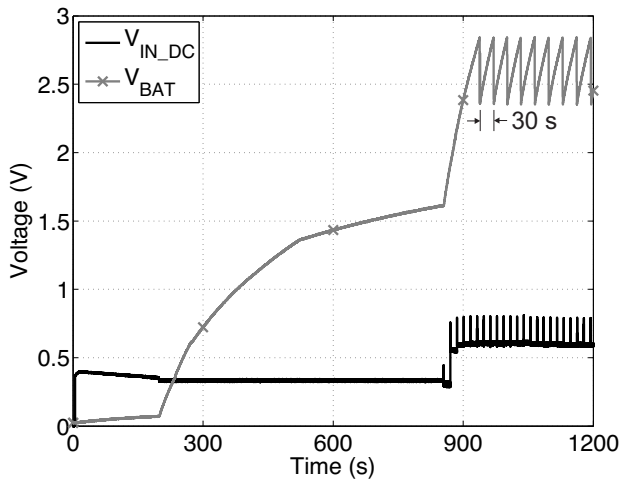
Next, the number of the rectennas were increased to three. For the same power density, the capacitor was charged after 679 s and the node operated every 22 s (Fig. 19(e)). Hence,
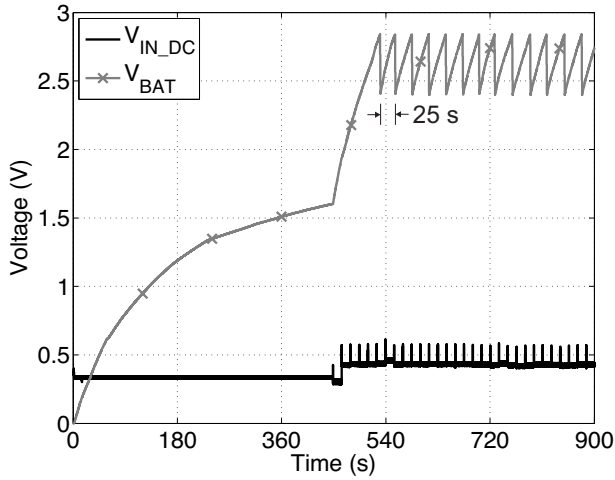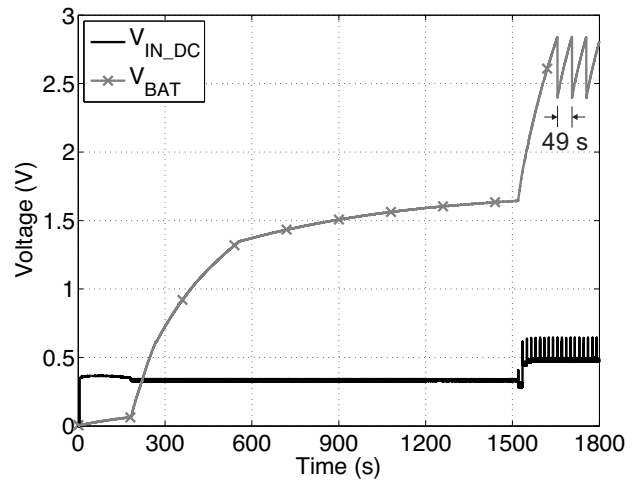
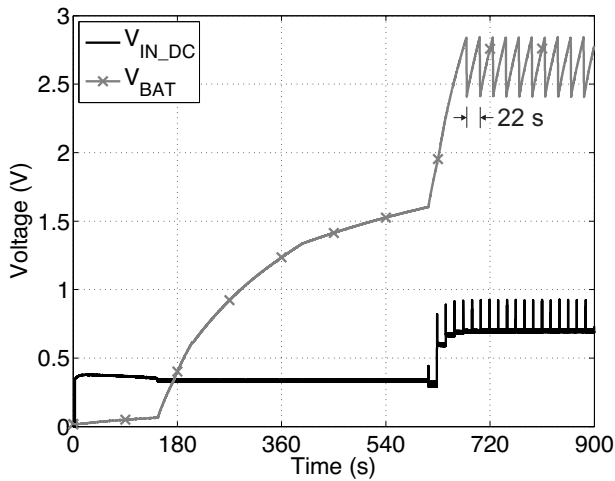(a) One rectenna (1×1 rectenna array) for $S = 0.1103 \ \mu\text{W/cm}^2$
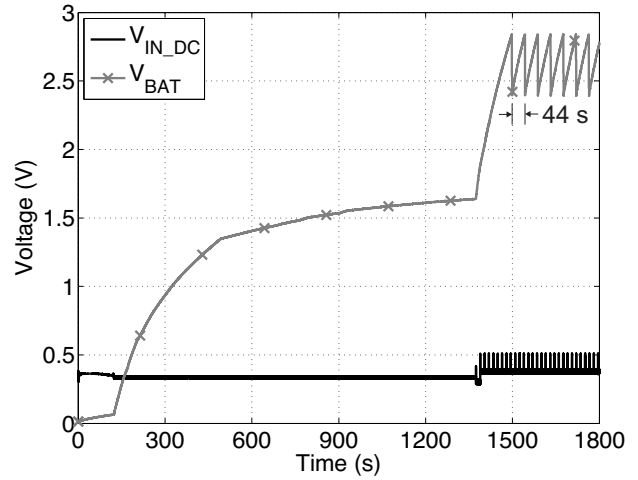
(b) One rectenna (1×1 rectenna array) for $S = 0.0876 \ \mu\text{W/cm}^2$
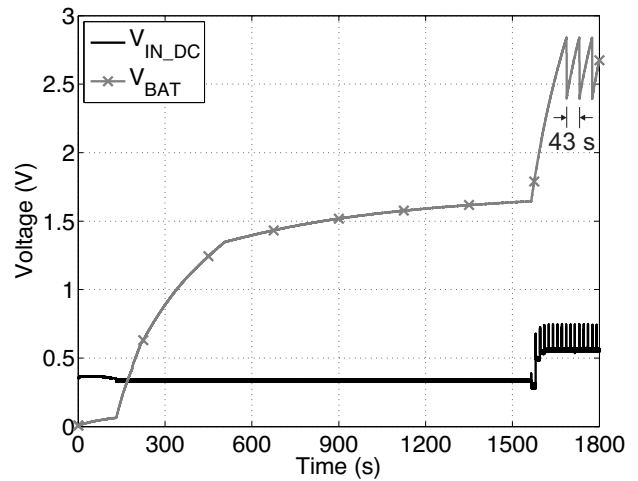
(c) Two rectennas (1×2 rectenna array) for $S = 0.0439 \ \mu\text{W/cm}^2$

(d) Two rectennas (1×2 rectenna array) for $S = 0.0220 \ \mu\text{W/cm}^2$

(e) Three rectennas (1×3 rectenna array) for $S = 0.0220 \ \mu\text{W/cm}^2$

(f) Three rectennas (1×3 rectenna array) for $S = 0.0139 \ \mu\text{W/cm}^2$

Fig. 19. Voltage across rectenna ouput (boost converter input $V_{\text{IN\_DC}}$) and 100 μF capacitor (boost converter output - V_{BAT}) for various levels of RF power density.
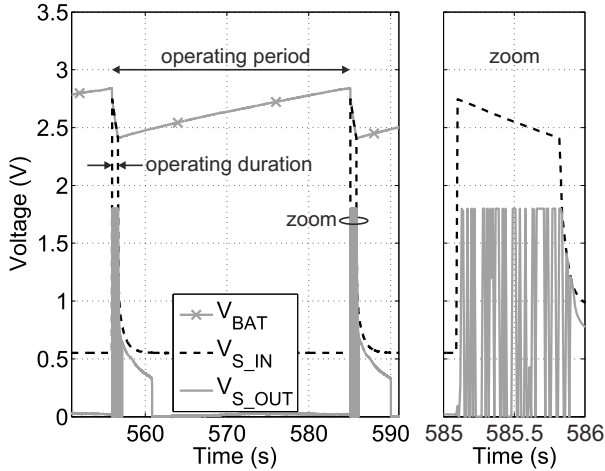
Fig. 20. Voltage across 100 μF capacitor (V_{BAT}), backscatter sensor node input ($V_{\text{S\_IN}}$) and output ($V_{\text{S\_OUT}}$) for one rectenna at $S = 0.1103\ \mu\text{W/cm}^2$ or equivalently for $P_{\text{cal}} = -18$ dBm.

the first time charging duration was decreased by a factor of 2.4 and the operating period by a factor of 2.2. It is noted that now $G = 6.43$ dB and thus $P_{\text{in}} = -20.37$ dBm. Then, power density was further decreased to $0.0139\ \mu\text{W/cm}^2$, corresponding to $P_{\text{cal}} = -27$ dBm and $P_{\text{in}} = -22.37$ dBm. The capacitor was charged after 1687 s, while the sensor operating period was 43 s (Fig. 19(f)). Again, it is emphasized that the boost converter was self-started and no external power was used for all the above cases. The latter was due to the fact that "bq25504" exhibits low cold start voltage (330 mV) and quiescent current (≤ 330 nA). At all cases where this boost converter was used, the above two requirements were fulfilled, hence there was no need for external energy support. For example, at the case with one rectenna and power input -19 dBm, rectenna efficiency is about 30%, offering maximum transferred power to boost converter of about 3.8 μW. According to Fig. 19(b), $V_{\text{IN\_DC}}$ is 360 mV, so maximum current input at boost converter is approximately 10.5 μA, which is much greater than lower quiescent current.

It is noted that for Fig. 19 different power density S levels (and equivalently power input P_{in}) were selected based on the measured power P_{cal} via the spectrum analyzer: P_{in} and power density S are obtained through (6), (7), given G_{cal}, while P_{cal} takes values from -18 to -27 dBm.

Fig. 20 depicts voltages V_{BAT}, $V_{\text{S\_IN}}$ and $V_{\text{S\_OUT}}$ for one operating period. For the shake of simplicity, only the case of one rectenna at $S = 0.1103\ \mu\text{W/cm}^2$ is presented (Fig. 19(a)). It is observed that the backscatter sensor node produces voltage squared pulses ($V_{\text{S\_OUT}}$) for 1 s (operating duration) every 25 s ("operating period"). The produced pulses are also shown. It is noted that the operating duration remains constant for all cases, while operating period varies, as already shown.

Finally, Figs. 21(a), 21(b) depict the first time charging duration and operating period, respectively, versus power density and size of rectenna array. It is observed that when the power density is decreased, both times are increased rapidly (i.e. logarithmically), as expected, while when power density
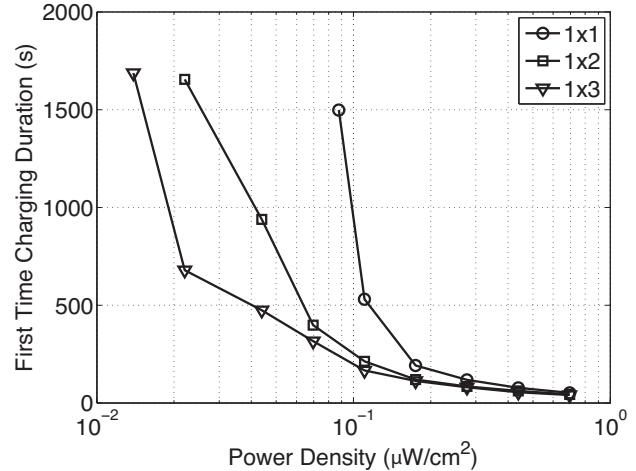
(a)
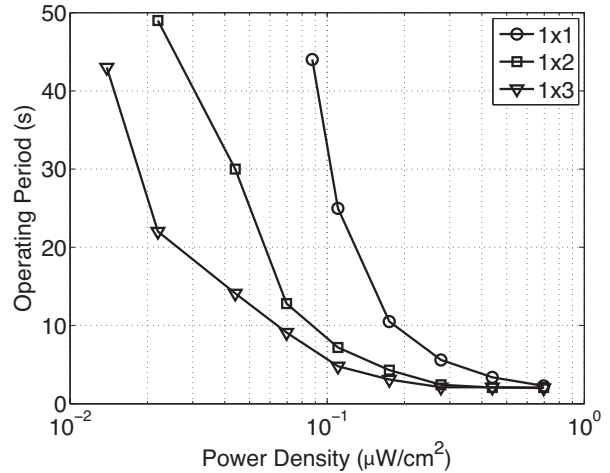
(b)

Fig. 21. First time charging duration (a) and operating period (b) vs power density for 1×1, 1×2 and 1×3 rectenna array.

is increased, e.g. for $S > 0.5\ \mu\text{W/cm}^2$, rectenna arrays have similar operation in terms of first time charging duration and operating period. At all cases, $V_{\text{IN\_DC}} \geq 330$ mV, so that the boost converter can start operating without any utilization of additional external power source. Hence, 1×1, 1×2 and 1×3 rectenna array starts capturing power when S is greater than 0.0876, 0.0220 and 0.0139 $\mu\text{W/cm}^2$, respectively. The fact that $V_{\text{IN\_DC}} \geq 330$ mV can be also observed at Fig. 19 for all illustrated cases.

V. CONCLUSION

This work presented the design, implementation and measurement of an efficient and sensitive RF harvesting supply, for low power input. The proposed low-complexity and cost rectifier system consists of a single series circuit with a double diode, on a low-cost, lossy FR-4 substrate. It was shown that rectifier microstrip trace dimensions are important optimization parameters, which could improve efficiency when addressed properly in the design methodology. Furthermore,

RF harvesting sensitivity can be increased using rectennas connected in series configuration and placed in specific topologies, forming rectenna arrays. In that way, sensor nodes can be powered even without commercial boost-converters. If the latter is utilized, sensitivity can be further increased, i.e. the supply can operate in smaller input power densities and specific duty-cycle scatter radio sensor examples were provided, requiring no other external power source.

Acknowledgment

References

[1] G. Vannucci, A. Bletsas, and D. Leigh, "A software-defined radio system for backscatter sensor networks," *IEEE Trans. Wireless Commun.*, vol. 7, no. 6, pp. 2170–2179, 2008.

[2] E. Kampianakis, S. D. Assimonis, and A. Bletsas, "Network demonstration of low-cost and ultra-low-power environmental sensing with analog backscatter," in *Proc. IEEE Topical Conf. on Wireless Sensors and Sensor Networks*, Newport Beach CA, USA, Jan. 2014, pp. 61–63.

[3] S.-N. Daskalakis, S. D. Assimonis, E. Kampianakis, and A. Bletsas, "Soil moisture wireless sensing with analog scatter radio, low power, ultra-low cost and extended communication ranges," in *Proc. IEEE Sensors Conf.*, Valencia, Spain, Nov. 2014.

[4] W. C. Brown, "The history of power transmission by radio waves," *IEEE Trans. Microw. Theory Techn.*, vol. 32, no. 9, pp. 1230–1242, 1984.

[5] J. Zbitou, M. Latrach, and S. Toutain, "Hybrid rectenna and monolithic integrated zero-bias microwave rectifier," *IEEE Trans. Microw. Theory Techn.*, vol. 54, no. 1, pp. 147–152, 2006.

[6] J. A. Hagerty, F. B. Helmbrecht, W. H. McCalpin, R. Zane, and Z. B. Popović, "Recycling ambient microwave energy with broad-band rectenna arrays," *IEEE Trans. Microw. Theory Techn.*, vol. 52, no. 3, pp. 1014–1024, 2004.

[7] J.-Y. Park, S.-M. Han, and T. Itoh, "A rectenna design with harmonic-rejecting circular-sector antenna," *IEEE Antennas Wireless Propag. Lett.*, vol. 3, no. 1, pp. 52–54, 2004.

[8] E. Falkenstein, M. Roberg, and Z. Popović, "Low-power wireless power delivery," *IEEE Trans. Microw. Theory Techn.*, vol. 60, no. 7, pp. 2277–2286, 2012.

[9] J. Akkermans, M. Van Beurden, G. Doodeman, and H. Visser, "Analytical models for low-power rectenna design," *IEEE Antennas Wireless Propag. Lett.*, vol. 4, pp. 187–190, 2005.

[10] R. J. Vyas, B. B. Cook, Y. Kawahara, and M. M. Tentzeris, "E-WEHP: A batteryless embedded sensor-platform wirelessly powered from ambient digital-TV signals," *IEEE Trans. Microw. Theory Techn.*, vol. 61, no. 6, pp. 2491–2505, 2013.

[11] A. N. Parks and J. R. Smith, "Sifting through the airwaves: Efficient and scalable multiband RF harvesting," in *Proc. IEEE Int. RFID Conf.*, Orlando FL, USA, Apr. 2014, pp. 74–81.

[12] A. Costanzo, A. Romani, D. Masotti, N. Arbizzani, and V. Rizzoli, "RF/baseband co-design of switching receivers for multiband microwave energy harvesting," *Sensors and Actuat. A: Phys.*, vol. 179, pp. 158–168, 2012.

[13] D. Masotti, A. Costanzo, P. Francia, M. Filippi, and A. Romani, "A load-modulated rectifier for RF micropower harvesting with start-up strategies," *IEEE Trans. Microw. Theory Techn.*, vol. 62, pp. 994–1004, 2014.

[14] H. Sun, Y.-x. Guo, M. He, and Z. Zhong, "Design of a high-efficiency 2.45-GHz rectenna for low-input-power energy harvesting," *IEEE Antennas Wireless Propag. Lett.*, vol. 11, pp. 929–932, 2012.

[15] A. Georgiadis, G. Andia, and A. Collado, "Rectenna design and optimization using reciprocity theory and harmonic balance analysis for electromagnetic (EM) energy harvesting," *IEEE Antennas Wireless Propag. Lett.*, vol. 9, pp. 444–446, 2010.

[16] A. Collado and A. Georgiadis, "Conformal hybrid solar and electromagnetic (EM) energy harvesting rectenna," *IEEE Trans. Circuits Syst. I*, vol. 60, no. 8, pp. 2225–2234, 2013.

[17] S. D. Assimonis and A. Bletsas, "Energy harvesting with a low-cost and high efficiency rectenna for low-power input," in *Proc. IEEE Radio Wireless Symposium*, Newport Beach CA, USA, Jan. 2014, pp. 229–231.

[18] S. D. Assimonis, S.-N. Daskalakis, and A. Bletsas, "Efficient RF harvesting for low-power input with low-cost lossy substrate rectenna grid," in *Proc. IEEE Int. RFID-Technol. Appl. Conf.*, Tampere, Finland, Sept. 2014, pp. 1–6.

[19] C. Mikeka, H. Arai, A. Georgiadis, and A. Collado, "DTV band micropower RF energy-harvesting circuit architecture and performance analysis," in *Proc. IEEE Int. RFID-Technol. Appl. Conf.*, Sitges, Spain, 2011, pp. 561–567.

[20] M. Piñuela, P. D. Mitcheson, and S. Lucyszyn, "Ambient RF energy harvesting in urban and semi-urban environments," *IEEE Trans. Microw. Theory Techn.*, vol. 61, no. 7, pp. 2715–2726, 2013.

[21] K. Gudan, S. Chemishkian, J. J. Hull, S. Thomas, J. Ensworth, and M. Reynolds, "A 2.4 GHz ambient RF energy harvesting system with -20 dBm minimum input power and NiMH battery storage," in *Proc. IEEE Int. RFID-Technol. Appl. Conf.*, Tampere, Finland, Sept. 2014, pp. 7–12.

[22] H. Reinisch, S. Gruber, H. Unterassinger, M. Wiessflecker, G. Hofer, W. Pribyl, and G. Holweg, "An electro-magnetic energy harvesting system with 190 nW idle mode power consumption for a BAW based wireless sensor node," *IEEE J. Solid-State Circuits*, vol. 46, no. 7, pp. 1728–1741, 2011.

[23] P. Nintanavongsa, U. Muncuk, D. R. Lewis, and K. R. Chowdhury, "Design optimization and implementation for RF energy harvesting circuits," *IEEE Trans. Emerg. Sel. Topics Circuits Syst.*, vol. 2, no. 1, pp. 24–33, 2012.

[24] A. Dolgov, R. Zane, and Z. Popović, "Power management system for online low power RF energy harvesting optimization," *IEEE Trans. Circuits Syst. I*, vol. 57, no. 7, pp. 1802–1811, Jul. 2010.

[25] T. Paing, E. A. Falkenstein, R. Zane, and Z. Popović, "Custom IC for ultra-low power RF energy harvesting," *IEEE Trans. Power Electron.*, vol. 26, no. 6, pp. 1620–1626, Jun. 2011.

[26] Z. Popović, E. A. Falkenstein, D. Costinett, and R. Zane, "Low-power far field wireless powering for wireless sensors," *Proc. IEEE*, vol. 101, no. 6, pp. 1397–1409, Jun. 2013, special Issue on Wireless Power Transmission, Technology & Applications.

[27] Z. Popović, S. Korhummel, S. Dunbar, R. Scheeler, A. Dolgov, R. Zane, E. Falkenstein, and J. Hagerty, "Scalable RF energy harvesting," *IEEE Trans. Microw. Theory Techn.*, vol. 62, no. 4, pp. 1046–1056, Apr. 2014.

[28] C. A. Balanis, *Antenna theory: analysis and design*. John Wiley & Sons, 2005, 3rd Edition.

[29] bq25504, "Ultra low-power boost converter with battery management for energy harvester applications," in *Texas Instruments SLUSAH0B Datasheet*, Oct. 2011, revised Dec. 2014.

Stylianos D. Assimonis was born in Thessaloniki, Greece. He obtained the Diploma/M.Eng. and Ph.D. degrees both in electrical and computer engineering from the Aristotle University of Thessaloniki (AUTh), Greece, in 2005 and 2011, respectively. From 2012 to 2015, he was with the Technical University of Crete (TUC) and the Radiocommunication Laboratory (RCL), in the School of Physics of AUTh, working as a Postdoctoral Researcher. He is currently a Senior Research Fellow at Queen's University Belfast, U.K.

His research interests span over a broad range of areas including Electromagnetics, Metamaterials, Antennas, RF Harvesting, Wireless Power Transfer, RF Sensing, and RF Front-End Design.

In 2012, he received the Postdoctoral Scholarship for Excellence from the Research Committee of AUTh, while he was the co-recipient of the Metamaterials' 2013 best paper award (3rd place), the 2014 IEEE RFID-TA best student paper competition finalist and the 2015 5th COST IC1301Workshop best student paper award (3rd prize).

Spyridon-Nektarios Daskalakis was born in Heraklion, Greece, in 1991. He received with excellence his Engineering Diploma in Electronic and Computer Engineering from Technical University of Crete (TUC) in 2014, and he is currently working toward the M.Sc. degree in the same department. His current research interests include low-cost wireless sensor networks and RF energy harvesting. Particularly he focuses on scatter radio networking, batteryless sensors, pcb design, low cost software defined radio, environmental sensing and RF energy harvesting design. He has received fellowship award for his project Aristeos (olive fly detection and monitoring with wireless sensor network) by the Clinton Global Initiative University 2014, Phoenix Arizona USA.

Aggelos Bletsas (S'03-M'05-SM'14) received with excellence his diploma degree in Electrical and Computer Engineering from Aristotle University of Thessaloniki, Greece in 1998, and the S.M. and Ph.D. degrees from Massachusetts Institute of Technology in 2001 and 2005, respectively. He worked at Mitsubishi Electric Research Laboratories (MERL), Cambridge MA, as a Postdoctoral Fellow and at Radiocommunications Laboratory (RCL), Department of Physics, Aristotle University of Thessaloniki, as a Visiting Scientist. He joined School of Electronic and Computer Engineering, Technical University of Crete, in summer of 2009, as an Assistant Professor, and promoted to Associate Professor at the beginning of 2014.

His research interests span the broad area of scalable wireless communication and networking, with emphasis on relay techniques, backscatter communications and RFID, energy harvesting, radio hardware/software implementations for wireless transceivers and low-cost sensor networks. His current vision and focus is on single-transistor front-ends and backscatter sensor networks, for LARGE-scale environmental sensing. He is the principal investigator (PI) of project BLASE: Backscatter Sensor Networks for Large-Scale Environmental Sensing, funded from the General Secretariat of Research & Technology Action Proposals evaluated positively from the 3rd European Research Council (ERC) Call. He is also Management Committee (MC) member and National Representative in the European Union COST Action IC1301 Wireless Power Transmission for Sustainable Electronics (WiPE). He is Associate Editor of IEEE Wireless Communication Letters since its foundation, Associate Editor of IEEE Transactions on Wireless Communications and Technical Program Committee (TPC) member of flagship IEEE conferences. He holds two patents from USPTO and he was recently included in https://sites.google.com/site/highlycited/highly-cited-greek-scientists.

Dr. Bletsas was the co-recipient of IEEE Communications Society 2008 Marconi Prize Paper Award in Wireless Communications, best paper distinction in ISWCS 2009, Siena, Italy, Second Best Student Paper Award in the IEEE RFID-TA 2011, Sitges, Barcelona, Spain, best paper distinction in IEEE Sensors Conference (SENSORS), November 2013, Baltimore, USA and best student paper award IEEE ICASSP 2015, April 2015, Brisbane, Australia. Two of his undergraduate advisees were winners of the 2009-2011 and 2011-2012 best Diploma Thesis contest, respectively, among all Greek Universities on "Advanced Wireless Systems", awarded by IEEE VTS/AES joint Greek Chapter. At the end of 2013, Dr. Bletsas was awarded the Technical University of Crete 2013 Research Excellence Award.